ANNEX VII

Second-Harmonic Operation of Coaxial Gyrotrons: Towards a Proof-of-Principle Experiment

K. A. Avramides[1], J. L. Vomvoridis[1], B. Piosczyk[2], and C. T. Iatrou[3]
[1]School of Electrical and Computer Engineering, National Technical University of Athens[2]Forschungszentrum Karlsruhe, IHM, Postfach 3640, D-76021 Karlsruhe, Germany
[3]Thales Electronic Systems, 48 Konstantinoupoleos Str., Koropi GR-19400, Greece

Theoretical analysis has shown that coaxial-cavity gyrotrons with a longitudinally corrugated insert are capable of powerful and efficient, continuous-wave (CW) operation at the second harmonic of the electron-cyclotron frequency [1]. The key factor is the remarkable mode selectivity that an appropriately designed coaxial cavity can exhibit. This selectivity makes feasible the second-harmonic excitation of a high-order TE mode with eigenvalue around 100, despite the high density of the spectrum of the competing modes. The experimental excitation of such a high-order, second-harmonic mode in a coaxial-cavity gyrotron will represent an important proof of the principle, since it will verify the predicted mode selectivity of the coaxial cavity, opening the way to efficient CW gyrotrons, able to deliver over 100 kW of submillimeter-wave radiation [1]. This experiment can be performed using (with minor modifications) the existing coaxial gyrotron for ITER at FZK, Germany.

EXISTING COAXIAL GYROTRON AND LIMITATIONS

The coaxial gyrotron for ITER is designed to operate with the co-rotating $TE_{34,19}$ mode (eigenvalue 105.2), resonant at the fundamental electron-cyclotron frequency, oscillating at about 170 GHz. At the operating point of 90 kV - 80 A, the output power is expected to exceed 2 MW. The coaxial cavity of this gyrotron is the one described as ITER in Table I, where the standard geometry parameters in cavity design are used [1].

Our major priority is to implement the second-harmonic experiment with the minimum number of changes in the existing facilities. In this respect, the frequency should be kept around 170 GHz since the RF output system and window are optimised for that frequency. Retaining the same outer wall radius of 29.55 mm, the operating mode can be $TE_{34,19}$ or another mode with similar eigenvalue. The second-harmonic excitation of such a high-order mode will suffice as proof of the principle. For second-harmonic operation at 170 GHz, the required magnetic field B_0 must be about half the magnetic field of 6.86 T of the ITER gyrotron. Consequently, the operating beam voltage V_b should also be reduced by a factor of 2 in order for the cathode to be able to produce an electron beam of good quality. Since the operating beam current scales as $I_b \sim V_b^{3/2}$, we focus on $B_0 \sim 3.4$ T, $V_b \sim 45$ kV, $I_b < 28$ A. The beam radius R_e cannot deviate much from the 10 mm beam radius of the ITER gyrotron. For a reasonable electron velocity ratio $\alpha \sim 1.3$ though, the anode has to be redesigned.

It would be attractive to excite the $TE_{34,19}$ mode as a second-harmonic mode in the ITER gyrotron cavity without any changes (apart from those on the operating parameters and the anode). Unfortunately, this does not seem possible according to the minimum starting currents, calculated according to [2], of the first-harmonic competing modes. Although the appropriate beam radius for best coupling was chosen, it seems that $TE_{34,19}$ will be suppressed by $TE_{-17,10}$ (we use a negative azimuthal index to denote a counter-rotating mode). The situation is expected to remain unfavourable for any other mode with similar eigenvalue and caustic radius. Obviously, $TE_{34,19}$ must get a lower relative starting current. This is possible by using a different corrugated insert, which will increase the mode's diffractive Q factor and decrease the diffractive Q factors of the first-harmonic competitors.

TABLE I
Coaxial-Cavity Geometries

	ITER	Cavity A	Cavity B
Cutoff section L_1 (mm)	22		
Midsection L_2 (mm)	16		24
Output section L_3 (mm)	20		12
Outer wall radius R_o (mm)*	29.55		
Input taper θ_1	3.0°		
Output taper θ_3	2.5°		
Inner rod radius R_i (mm)*	7.86	9.06	8.79
Inner rod taper θ_{in}**	1.0° down-tapered		
Number of corrugations N	75		
Corrugation period s (mm)*	0.66	0.76	0.74
Slot width to period l/s	0.5		
Corrugation depth d (mm)	0.44	0.88	0.70

* *At the middle of the midsection*
** *In Cavity B the taper begins at the midsection*

MODIFIED COAXIAL GYROTRON

The choice of the corrugation depth that is more suitable for CW second-harmonic operation is $d/\lambda = 0.4$ where λ is the free-space wavelength of the operating mode [1]. However, within the limitations of the present case, the choice $d/\lambda = 0.4$ results in a minimum starting current above 60 A for the $TE_{34,19}$ mode. This means that $TE_{34,19}$ cannot be excited with the available beam parameters, so its diffractive Q factor should be further increased. This is done by choosing $d = 0.88$ mm which gives $d/\lambda = 0.5$ for the $TE_{34,19}$ mode. We use a down-

tapered insert with a radius that corresponds to the cavity C ($C = R_o/R_i$) at which the eigenvalue curve (eigenvalue versus C) of $TE_{34,19}$ exhibits the steepest positive slope [3]. The resulting cavity configuration is presented in Table I as Cavity A. The starting current curves in Cavity A (for realistic field profiles of the modes) are shown in Fig. 1(a). The counter-rotating $TE_{-34,19}$ mode has been employed because the co-rotating one would require a beam radius of 9.5 mm which is too close to the inner conductor's surface. The beam-current curve indicates that $TE_{-34,19}$ will be the only mode to oscillate during the diode start-up. The performance of this modified ITER gyrotron has been simulated by a time-dependent, fixed-field code and is summarised in Table II for two cases: The case of the maximum permissible beam current $I_b = 28$ A, resulting (for short-pulse operation) in the maximum efficiency (3 %), and the case of $I_b = 25.8$ A where the CW requirements for the ohmic loading of the insert (≤ 0.1 kW/cm^2) are met.

In Table II, $\eta_{el} = [\alpha^2/(1+\alpha^2)]\eta_\perp$ and $\eta_{tot} = (1-\Delta V)(Q_{tot}/Q_{dif})\eta_{el}$ with $\Delta V = (V_c - V_b)/V_c$, V_c being the cathode voltage. The total efficiency η_{tot} is defined as the ratio of the RF power P_{out} delivered at the cavity output to the product $I_b V_c$. The conclusion from Table II is that the efficiency remains at low levels. This is so because the normalised field amplitude F is very small (< 0.015) and at the same time the normalised cavity length μ is also relatively small ($\mu \sim 14$) [2]. To improve the efficiency, we can increase F by using a larger diffractive Q factor, via deeper corrugations ($d/\lambda = 0.6$) [1]. However, only pulsed operation can be targeted in this way because the ohmic loading of the insert will increase. A better way to improve the efficiency is the use of a longer midsection.

In a cavity with a longer midsection, the larger μ-values reduce the starting currents of all the modes. It is thus not necessary to help the operating mode by increasing substantially its diffractive Q factor via a corrugation depth of $d/\lambda = 0.5$. We can just use $d/\lambda = 0.4$. Thus, the ohmic wall loading of the insert is expected to decrease, permitting CW operation with larger output power. Extended tests showed that the $TE_{34,19}$ mode as a second-harmonic mode in such a cavity was suppressed by $TE_{17,10}$, the first-harmonic competitor. As a result, the cavity was designed to favour the excitation of the $TE_{35,19}$ mode, which does not face such competition. This cavity is described in Table I as Cavity B. It exhibits a midsection 50 % longer than the midsection of the ITER cavity, while it retains the same total length of 58 mm. The pertinent starting current curves are shown in Fig. 1(b). Again, only the operating $TE_{35,19}$ mode will oscillate during the diode start-up. The performance of this design is presented in Table II. Even for the maximum operating current (28 A) the CW limitations for the ohmic loading are satisfied. Clearly, with a longer midsection, the efficiency and output power are significantly increased.

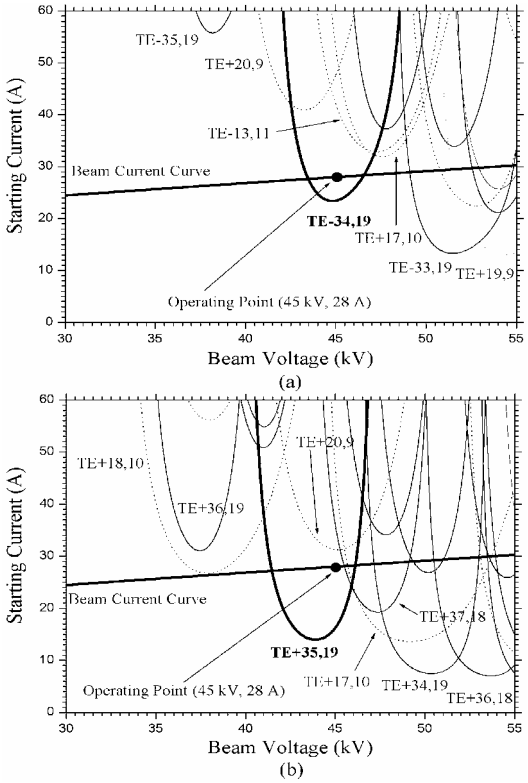

Fig. 1: Starting currents versus the beam voltage. The solid (dotted) curves denote second- (first-) harmonic modes. (a) Cavity A with $B_0 = 3.243$ T. (b) Cavity B.

TABLE II
Operating Parameters and Calculated Performance

	Cavity A		Cavity B
	Max. I_b	CW	CW
Magnetic field B_0 (T)	3.243	3.245	3.291
Operating mode	$TE_{-34,19}$		$TE_{+35,19}$
Operating frequency f (GHz)	169.57	169.58	172.04
Diffractive Q factor Q_{dif}	3820		4740
Ohmic Q factor Q_{ohm}*	44500		134600
Beam radius R_e (mm)	10.64		9.87
Beam voltage V_b (kV)	45		
Beam current I_b (A)	28	25.8	28
Electron velocity ratio α	1.3		
Output power P_{out} (kW)	38.9	22.6	206.8
Ohmic losses, wall (kW)*	0.8	0.5	6.0
Ohmic losses, insert (kW)*	2.5	1.4	1.3
Outer wall loading (kW/cm^2)*	0.03	0.02	0.2
Inner rod loading (kW/cm^2)*	0.2	0.1	0.1
Voltage depression ΔV	2.0 %	1.8 %	1.5 %
Transverse efficiency $\eta_\perp$	5.3 %	3.3 %	27.0 %
Electronic efficiency η_{el}	3.3 %	2.1 %	17.0 %
Ohmic losses $1 - Q_{tot}/Q_{dif}$*	7.9 %		3.4 %
Total efficiency η_{tot}*	3.0 %	1.9 %	16.2 %

**At room temperature (conductivity 5.7×10^7 S/m)*

REFERENCES

[1] K. A. Avramides et al., IEEE Trans. Plasma Sci., vol. 32, no. 3, pp. 917-928, June 2004.
[2] B. G. Danly et al., Phys. Fluids vol. 29, no. 2, pp. 561-567, February 1986.
[3] C. T. Iatrou et al., IEEE Trans. Microwave Theory Tech., vol. 44, no. 1, pp. 56-64, January 1996.